Aalto University

OPEN ACCESS

This is an electronic reprint of the original article.
This reprint may differ from the original in pagination and typographic detail.

Hancock, Y.; Uppstu, A.; Saloriutta, K.; Harju, A.; Puska, M.J.

Generalized tight-binding transport model for graphene nanoribbon-based systems

Published in:
Physical Review B

DOI:
10.1103/PhysRevB.81.245402

Published: 01/06/2010

Document Version
Publisher's PDF, also known as Version of record

Please cite the original version:
Hancock, Y., Uppstu, A., Saloriutta, K., Harju, A., & Puska, M. J. (2010). Generalized tight-binding transport model for graphene nanoribbon-based systems. *Physical Review B*, *81*(24), 1-6. [245402]. https://doi.org/10.1103/PhysRevB.81.245402

This material is protected by copyright and other intellectual property rights, and duplication or sale of all or part of any of the repository collections is not permitted, except that material may be duplicated by you for your research use or educational purposes in electronic or print form. You must obtain permission for any other use. Electronic or print copies may not be offered, whether for sale or otherwise to anyone who is not an authorised user.

Generalized tight-binding transport model for graphene nanoribbon-based systems

Y. Hancock,[1,2,*] A. Uppstu,[1] K. Saloriutta,[1] A. Harju,[1,3] and M. J. Puska[1]
[1]*Department of Applied Physics, Aalto University, School of Science and Technology, P.O. Box 11100, FIN-00076 AALTO, Finland*
[2]*Department of Physics, The University of York, York YO10 5DD, United Kingdom*
[3]*Helsinki Institute of Physics, Aalto University, School of Science and Technology, P.O. Box 11100, FIN-00076 AALTO, Finland*
(Received 30 January 2010; revised manuscript received 6 April 2010; published 1 June 2010)

An extended tight-binding model that includes up to third-nearest-neighbor hopping and a Hubbard mean-field interaction term is tested against *ab initio* local spin-density approximation results of band structures for armchair- and zigzag-edged graphene nanoribbons. A single tight-binding parameter set is found to accurately reproduce the *ab initio* results for both the armchair and zigzag cases. Transport calculations based on the extended tight-binding model faithfully reproduce the results of *ab initio* transport calculations of graphene nanoribbon-based systems.

DOI: 10.1103/PhysRevB.81.245402 PACS number(s): 73.22.Pr, 72.80.Vp, 71.10.Fd, 73.63.−b

I. INTRODUCTION

Graphene nanoribbons (GNRs) are quasi-one-dimensional graphene strips of nanometer width that are considered to be important building blocks for future carbon-based electronics (Fig. 1).[1] Experiments show that GNRs are semiconductors with band gaps that scale inversely against the nanoribbon width.[2,3] The band gaps of GNRs also depend on other factors, such as the edge shape[4] and the addition of functional groups at the nanoribbon edge.[5] The tunability of the band gap through width- and edge-dependent properties allows for the potential to design and manufacture a diverse range of GNR-based devices.[1,6,7]

The simple tight-binding (TB) model with only nearest-neighbor hopping has been widely used to describe the physics of GNRs.[4,8] Recently, much effort has focused on determining extended TB models that can accurately reproduce the band gaps and band structures of GNRs obtained from computationally demanding *ab initio* calculations. For example, the band structure of armchair GNRs (AGNRs) can be modeled by introducing third-nearest-neighbor hopping and perturbation to the edge hopping as additional features into the TB model.[8–10] Whereas, zigzag GNRs (ZGNRs) can be described using a mean-field Hubbard model, which predicts a band gap, well-defined edge state, and antiferromagnetic alignment of the spins across the edges of the ribbon.[11–14]

The aim of this work is to present a generalized, extended TB model for GNR-based systems. The effect of extended hoppings, a mean-field Hubbard U interaction and orbital overlaps on the TB band structures are systematically compared against *ab initio* local spin-density approximation (LSDA) results. The LSDA was chosen as this is expected to give a good first approximation to the qualitative features of the experimentally observed band gaps of GNRs, particularly those with widths of 20 nm or less.[2,3,6] Although the GW approximation improves upon the quantitative features of the GNR band gaps,[15] we prefer in this case to fit our TB parameters to the LSDA, which can model a broader range of systems and has also been adapted for electron transport calculations.

The TB model is computationally efficient against *ab initio* calculations and can be easily modified to include structural imperfections, patterning, and other realistic features. To test the applicability of the generalized TB model, conductances of notched, GNR-based systems are calculated within the Landauer-Büttiker transport formalism,[16] and compared against *ab initio* transport theory[17] predictions. The successful application of a generalized TB model and TB-based transport method would mean improved computational efficiency for estimating the properties of graphene-based, low-symmetry systems that are of interest for future device applications.

II. GENERALIZED TB MODEL FOR GNRs

A. Theoretical method

Following the standard convention, AGNRs are labeled based on the number of dimer lines located along the width of the ribbon (N_a), while ZGNRs are labeled based on the number of zigzag chains across the ribbon width (N_z) (Fig. 1). An AGNR (ZGNR) whose width is $N_A(N_Z)$ is called N_A-AGNR (N_Z-ZGNR). The computational unit cells, with unit cell widths, a for the AGNR and z for the ZGNR, are also shown. To model the GNRs, a single-band, mean-field Hubbard Hamiltonian with extended hoppings is used to describe the π-electron structure. The edges of the GNR are considered to be hydrogen passivated, which affects only the sp^2 bonding, and has little effect on the π bonds. Hence, within the TB description, the edge carbon atoms are treated in the same way as the bulk carbon atoms, with only a small perturbation to the edge hopping.[18,19]

Written in second quantization representation, the Hamiltonian is

$$\boldsymbol{H} = -\sum_{ij\sigma} (t_{ij} c_{i\sigma}^{\dagger} c_{j\sigma} + \text{H.c.}) + U \sum_{i} (n_{i\uparrow}\langle n_{i\downarrow}\rangle + n_{i\downarrow}\langle n_{i\uparrow}\rangle - \langle n_{i\uparrow}\rangle\langle n_{i\downarrow}\rangle), \quad (1)$$

where $c_{i\sigma}^{\dagger}$ and $c_{i\sigma}$ are the fermion creation and annihilation operators, respectively, and $n_{i\sigma}$ is the number operator at site i. The spin is denoted by $\sigma=\uparrow$ or $\downarrow$. The hopping integral, t_{ij}, is taken up to third-nearest-neighbor, with t_1 for nearest-

 ©2010 The American Physical Society

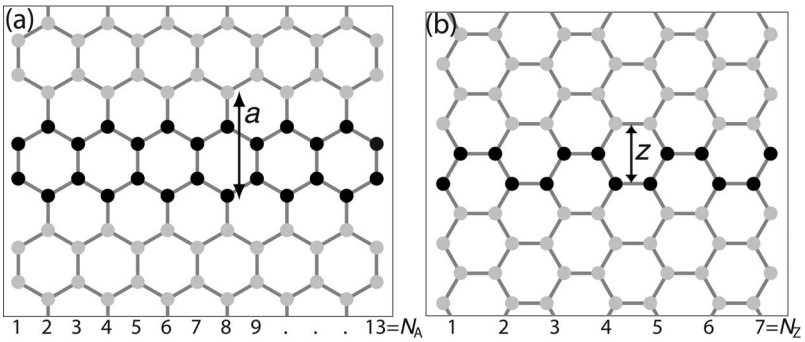

FIG. 1. Labeling conventions for (a) an armchair nanoribbon (13-AGNR) and (b) a zigzag nanoribbon (7-ZGNR). The computational unit cells and unit cell widths of a for AGNRs and z for ZGNRs are highlighted.

neighbor, t_2 for next-nearest-neighbor, and t_3 for third-nearest-neighbor hoppings. The on-site Coulomb repulsion between electrons of opposite spin is denoted by the Hubbard U. In applying the mean-field approximation,

$$\langle n_{i\sigma}\rangle = -\frac{1}{\pi}\int_{-\infty}^{E_F} \mathrm{Im}(G^R_{\sigma ii})dE \tag{2}$$

are the average spin-dependent local occupancies and $G^R_{\sigma ii}$ are the diagonal elements of the retarded Green's function. Equation (1) can be decoupled into two linear spin-dependent Hamiltonians $\boldsymbol{H}_{\sigma=\uparrow,\downarrow}$ that are solved self-consistently starting from the $U=0$ paramagnetic solution.[20]

The overlap between basis states centered on different lattice sites can also be taken into account through an overlap matrix $\boldsymbol{S}_\sigma$, which changes the eigenvalue problem to

$$\boldsymbol{H}_\sigma|\psi\rangle^\alpha_\sigma = \epsilon_\alpha \boldsymbol{S}_\sigma|\psi\rangle^\alpha_\sigma. \tag{3}$$

Here,

$$|\psi\rangle^\alpha_\sigma = \sum_i a^\alpha_{i\sigma}|i\rangle_\sigma \tag{4}$$

is the αth spin-dependent, single-particle eigenstate expanded as a linear combination of local basis states, $|i\rangle_\sigma$. The elements of $\boldsymbol{S}_\sigma$ are

$$S_{ij\sigma} = {}_\sigma\langle i|j\rangle_\sigma, \tag{5}$$

where, $S_{ij\sigma}=s_1$ for nearest-neighbors, s_2 for next-nearest-neighbors, s_3 for third-nearest-neighbors, and $S_{ij\sigma}=0$ for greater than third-nearest-neighbor separations. In the case of overlap, the average local spin occupation can be obtained from

$$\langle n_{i\sigma}\rangle = \sum_j S_{ij\sigma}\rho_{ij\sigma}, \tag{6}$$

where $\rho_{ij\sigma}$ is the spin-dependent density-matrix element,

$$\rho_{ij\sigma} = \sum_{\alpha=1}^{occup.} {}_\sigma\langle i|\psi\rangle^{\alpha\alpha}_{\sigma\sigma}\langle\psi|j\rangle_\sigma. \tag{7}$$

The extended TB model [Eq. (1)] was fitted against the band structure and gap results obtained from self-consistent pseudopotential calculations using the SIESTA implementation of the density-functional theory (DFT).[21,22] The LSDA is applied, as well as the double zeta plus polarization (DZP) basis set and a 400 Ry real-space grid cutoff. A 0.01 eV/Å force tolerance is set on the atoms during relaxation. Given the large number of fitted parameters, we chose to fit the TB model by inspection, and in doing so do not attribute any strict physical meaning to the parameters, but rather consider them to be fitted variables, similar to Ref. 23.

B. Band-structure comparison

Rows A–F in Fig. 2 compare the TB band structures and band-gap widths of ZGNRs and AGNRs from the parameter sets in Table I against the LSDA results. Note that parameter set E (Table I) includes an edge perturbation to the nearest-neighbor hopping parameters, $t_{edge,a}$ and $t_{edge,z}$, for the AGNR and ZGNR edge atoms, respectively. Also, parameter set F includes the overlap parameterization, s_1, s_2, and s_3.

In rows A–E (Fig. 2), the TB and *ab initio* comparisons for the ZGNR system (columns 1 and 2) are shown to be sensitive to the Hubbard U, the t_2 particle-hole symmetry-breaking term, and t_3, whereas the AGNR comparisons (columns 3 and 4) are sensitive to the t_3 term and to the perturbation to the edge hopping, $t_{edge,a}$. The value of $U=2$ eV has been obtained by fitting to the *ab initio* gap results of the ZGNR.

The trends shown in Fig. 2 and the values of our fitted parameters in Table I are in general agreement with previously published work.[8–14] What is unique to this study, however, is that we show that a single TB parameter set can be used to model both AGNR and ZGNR systems. Without edge-hopping perturbation, the combination of the required AGNR and ZGNR parameters leads to a minimal, generalized TB model (set D, Table I) that adequately reproduces the band-structure features about the Fermi energy and gap trends of the *ab initio* results—note that the gaps for both the AGNR and ZGNR have been adequately obtained using the t_3 term (see also Refs. 10 and 14) and the Hubbard U, respectively. The generalized TB model has important consequences, as realistic graphene devices require modeling of nontrivial structures that have a mixture of AGNR and ZGNR edges.

The inclusion of the overlap parameters from set F in Table I produces an accurate reproduction of the full LSDA band structures and gap widths for both the ZGNR and AGNR systems, even without the edge-hopping perturbation (row F, Fig. 2). Interestingly, a similar parameter set, without the Hubbard U, was also found for bulk graphene and carbon nanotubes (cf. parameter sets F and G in Table I). Although edge perturbation (row E, Fig. 2) and overlaps (row F, Fig. 2) improve the quantitative features of the TB and *ab initio*

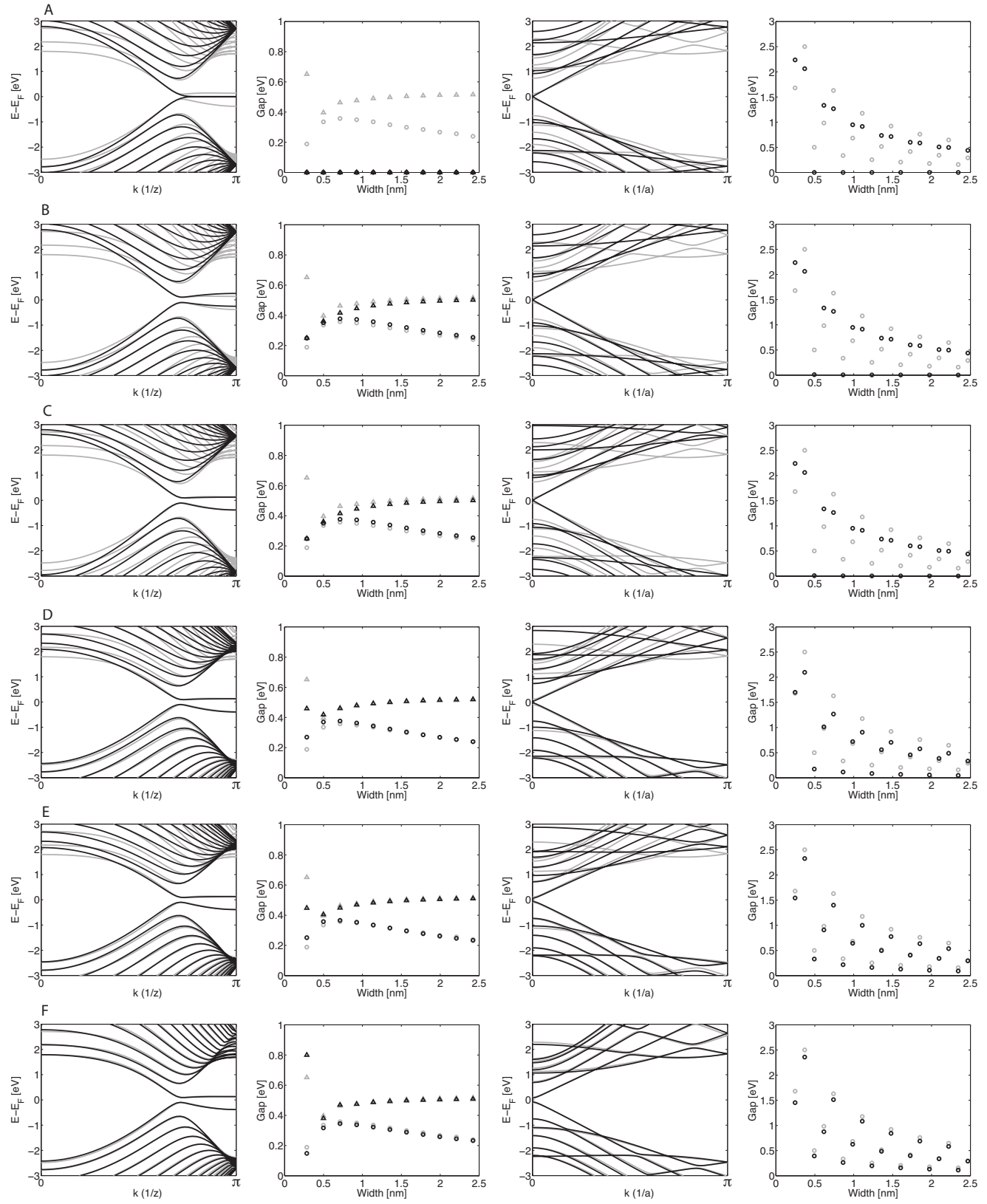

FIG. 2. Band structures and band gaps of ZGNRs (image columns 1 and 2—left) and AGNRs (image columns 3 and 4—right) calculated using different TB parameter sets, rows A–F (Table I), with row F including the orbital overlap. The TB results are black with the corresponding *ab initio* results in the background (gray). The band structures were calculated for 16-ZGNR (3.3-nm-width ribbon) and 14-AGNR (1.6-nm-width ribbon) systems. The band-structure energies are taken relative to the Fermi energy, E_F. The ZGNR band-gap results show the energy splittings at $kz=\pi$ (marked with "△"s) in addition to the direct band gaps (marked with "o"s).

TABLE I. TB parameter sets in units of electron volt. G=bulk graphene and carbon nanotubes, Ref. 23.

Set	t_1	t_2	t_3	s_1	s_2	s_3	U	$t_{edge,a}$	$t_{edge,z}$
A	2.7	0.0	0.0	0.0	0.0	0.0	0.0	t_1	t_1
B	2.7	0.0	0.0	0.0	0.0	0.0	2.0	t_1	t_1
C	2.7	0.2	0.0	0.0	0.0	0.0	2.0	t_1	t_1
D	2.7	0.2	0.18	0.0	0.0	0.0	2.0	t_1	t_1
E	2.7	0.2	0.18	0.0	0.0	0.0	2.0	$1.06t_1$	$1.03t_1$
F	2.7	0.09	0.27	0.11	0.045	0.065	2.0	t_1	t_1
G	2.97	0.073	0.33	0.073	0.018	0.026	0.0	t_1	t_1

comparison, it is sufficient to choose the minimal parametrization for the generalized TB model—thus for the transport calculations in Sec. III, the parameter set in D (Table I) is selected.

III. TRANSPORT CALCULATIONS

A. Theoretical method

Assuming coherent transport, the conductance through GNR-based systems having GNR leads can be calculated using the Landauer-Bütticker formalism.[16] The spin-dependent electronic conductances, $G_\sigma(E)$, at energy E, are calculated from the transmission function, $T_\sigma(E)$, where

$$G_\sigma(E) = \frac{e^2}{h} T_\sigma(E). \tag{8}$$

Here,

$$T_\sigma(E) = \mathrm{Tr}[\Gamma_{\mathrm{L}\sigma}(E) G^R_\sigma(E) \Gamma_{\mathrm{R}\sigma}(E) G^A_\sigma(E)], \tag{9}$$

where $G^{R/A}_\sigma(E)$ are the retarded/advanced Green's functions. The Γ matrices for the left (L) and right (R) leads, $\Gamma_{\mathrm{L/R}\sigma}(E)$, are obtained from

$$\Gamma_{\mathrm{L/R}\sigma}(E) = i[\Sigma^R_{\mathrm{L/R}\sigma}(E) - \Sigma^A_{\mathrm{L/R}\sigma}(E)], \tag{10}$$

where

$$\Sigma^{R/A}_{\mathrm{L/R}\sigma}(E) = V^\dagger_{\mathrm{L/R\ }sys} g^{R/A}_{L/R}(E) V_{\mathrm{L/R\ }sys} \tag{11}$$

are the retarded/advanced self-energies. Here, $V_{\mathrm{L/R\ }sys}$ describes the coupling between the GNR-based system and the L/R lead and $g^{R/A}_{\mathrm{L/R}}(E)$ are the retarded/advanced surface Green's functions for the leads. The surface Green's functions for the leads [required in Eq. (11)] are obtained using the decimation iteration method.[24] To calculate the transmission functions [Eq. (10)], the procedure in Ref. 25 is followed.

The Hubbard term in Eq. (1) requires additional computational effort as the average spin occupancies [Eq. (2)] are solved self-consistently for the device region. Consequently, to ensure a continuous density distribution, the device region needs to include long enough parts of the defect-free (i.e., ideal) GNR leads.

The conductances from the extended TB model [Eq. (8)] are compared against *ab initio* results using the TRANSIESTA code,[17] which applies a nonequilibrium Green's-function formalism to the SIESTA DFT method.[21,22] In the *ab initio* calculations, the DZP basis set and a 275 Ry energy cutoff are used within the LSDA. The system is hydrogen passivated with a C-H distance of 1.126 Å and a C-C distance of 1.422 Å. The ionic degrees of freedom are not relaxed for the transport calculation. The local spin polarizations

$$p_i = \frac{\langle n_{i\sigma}\rangle - \langle n_{i-\sigma}\rangle}{\langle n_{i\sigma}\rangle + \langle n_{i-\sigma}\rangle} \tag{12}$$

are also calculated from the TB model.

B. Transport comparison

A test case for the generalized TB model is the proposed ZGNR-notched system of Wimmer *et al.*[26] [Fig. 3(a)]. To further demonstrate the application of this model, an AGNR-notched device is also chosen [Fig. 3(b)]. Both of these mixed-edge systems have sufficient structural complexity, thereby making these reasonable tests for the generalized TB description (for the single-edge-type GNR comparison see Ref. 27).

The local spin polarizations from the TB model are shown in Fig. 3. The notched ZGNR is strongly spin dependent at the edges of the system, whereas the notched AGNR is nonmagnetic. The TB conductances for both systems were cal-

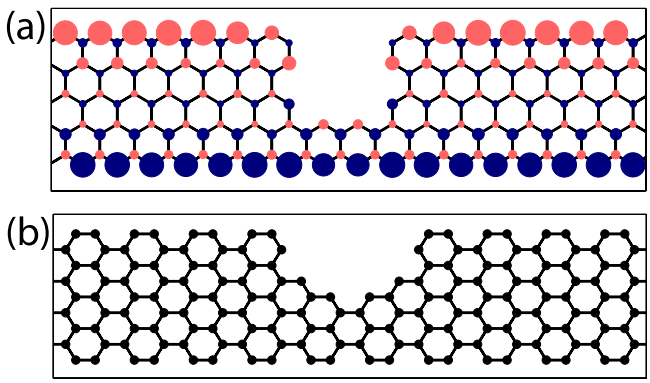

FIG. 3. (Color online) Asymmetric notched (a) ZGNR and (b) AGNR systems selected for the transport comparison between the extended TB and the *ab initio* calculations. The notched ZGNR exhibits spin polarization across the edges of the ribbon with dark (blue)=spin up and light (red)=spin down. The notched AGNR is nonmagnetic.

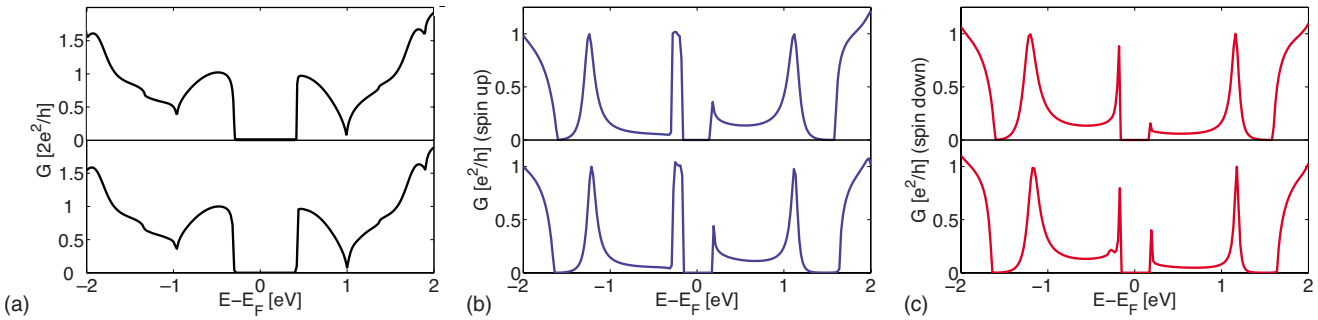

FIG. 4. (Color online) A comparison of transport results from the *ab initio* model (lower row) and the extended TB model (upper row), calculated with parameter set D from Table I. The conductance of the notched AGNR (a) is spin independent, whereas the conductance of the notched ZGNR is spin dependent, as shown by the spin-up (blue) and spin-down (red) conductances in (b) and (c), respectively.

culated using the minimal model (parameter set D, Table I). Comparison with the TRANSIESTA *ab initio* results (Fig. 4) shows that the TB transport model faithfully reproduces the essential conductance features of both of these systems. The notched AGNR does not exhibit spin polarization, hence the transmission for this system is spin independent [Fig. 4(a)]. The notch in the ZGNR, however, breaks the symmetry of the spin polarization of the edge states and results in spin-dependent transmission [Figs. 4(b) and 4(c)]. Notched ZGNRs have been proposed as a basis for spintronic devices[26] assuming that a small voltage bias does not destroy the spin polarization, and therefore change the conductance.[14]

We are working toward extending the generalized TB transport model to take into account more energetically favorable, reconstructions of the hydrogen-passivated GNR edges.[28] As the Hubbard model has been successfully applied to quantum-dot systems,[29] we are also investigating the applicability of the extended TB model in explaining resonance signatures and larger conductance gaps, which are believed to result from quantum-dot behavior in notched GNRs.[30]

IV. CONCLUSION

A generalized TB model has been proposed for nontrivially shaped GNR-based systems. The transport results obtained from this model faithfully reproduce *ab initio* transport simulations. The application of a generalized TB transport method would mean more realistic and computationally efficient modeling of low-symmetry, GNR-based systems.

ACKNOWLEDGMENTS

We acknowledge financial support from the Academy of Finland through its Center of Excellence Program (2006-11). We thank Antti-Pekka Jauho for helpful discussions and Mads Brandbyge for his help with, and permission to use the TRANSIESTA code. We also gratefully acknowledge fruitful discussions with members of the Nokia-TKK collaboration. The Center for Scientific Computing (CSC) have assisted us with their computing resources, and we are thankful for their continuing support. We would also like to thank David Schultz for his assistance with formatting the figures.

*yh546@york.ac.uk

[1] P. Avouris, Z. Chen, and V. Perebeinos, Nat. Nanotechnol. **2**, 605 (2007).
[2] M. Y. Han, B. Özyilmaz, Y. Zhang, and P. Kim, Phys. Rev. Lett. **98**, 206805 (2007).
[3] X. Li, X. Wang, L. Zhang, S. Lee, and H. Dai, Science **319**, 1229 (2008).
[4] K. Nakada, M. Fujita, G. Dresselhaus, and M. S. Dresselhaus, Phys. Rev. B **54**, 17954 (1996).
[5] Z. F. Wang, Q. Li, H. Zheng, H. Ren, H. Su, Q. W. Shi, and J. Chen, Phys. Rev. B **75**, 113406 (2007).
[6] Z. Chen, Y.-M. Lin, M. J. Rooks, and P. Avouris, Physica E **40**, 228 (2007).
[7] X. Wang, Y. Ouyang, X. Li, H. Wang, J. Guo, and H. Dai, Phys. Rev. Lett. **100**, 206803 (2008).
[8] Y.-W. Son, M. L. Cohen, and S. G. Louie, Phys. Rev. Lett. **97**, 216803 (2006).
[9] C. T. White, J. Li, D. Gunlycke, and J. W. Mintmire, Nano Lett. **7**, 825 (2007).
[10] D. Gunlycke and C. T. White, Phys. Rev. B **77**, 115116 (2008).
[11] K. Wakabayashi, in *Carbon-Based Magnetism: An Overview of the Magnetism of Metal Free Carbon-Based Compounds and Materials*, edited by T. Makarova and F. Palacio (Elsevier, New York, 2007), pp. 279–304.
[12] A. Yamashiro, Y. Shimoi, K. Harigaya, and K. Wakabayashi, Phys. Rev. B **68**, 193410 (2003).
[13] J. Fernández-Rossier, Phys. Rev. B **77**, 075430 (2008).
[14] D. Gunlycke, D. A. Areshkin, J. Li, J. W. Mintmire, and C. T. White, Nano Lett. **7**, 3608 (2007).
[15] L. Yang, C.-H. Park, Y.-W. Son, M. L. Cohen, and S. G. Louie, Phys. Rev. Lett. **99**, 186801 (2007).
[16] S. Datta, *Electronic Transport in Mesoscopic Systems* (Cambridge University Press, Cambridge, England, 1997).
[17] M. Brandbyge, J.-L. Mozos, P. Ordejón, J. Taylor, and K. Stokbro, Phys. Rev. B **65**, 165401 (2002).
[18] D. A. Areshkin, D. Gunlycke, and C. T. White, Nano Lett. **7**, 204

(2007).
[19] J. Akola, H. P. Heiskanen, and M. Manninen, Phys. Rev. B **77**, 193410 (2008).
[20] Y. Hancock and A. E. Smith, Physica E **18**, 383 (2003).
[21] J. M. Soler, E. Artacho, J. D. Gale, A. García, J. Junquera, P. Ordejón, and D. Sánchez-Portal, J. Phys.: Condens. Matter **14**, 2745 (2002).
[22] P. Ordejón, E. Artacho, and J. M. Soler, Phys. Rev. B **53**, R10441 (1996).
[23] S. Reich, J. Maultzsch, C. Thomsen, and P. Ordejón, Phys. Rev. B **66**, 035412 (2002).
[24] F. Guinea, C. Tejedor, F. Flores, and E. Louis, Phys. Rev. B **28**, 4397 (1983).
[25] F. Muñoz-Rojas, D. Jacob, J. Fernandez-Rossier, and J. J. Palacios, Phys. Rev. B **74**, 195417 (2006).
[26] M. Wimmer, I. Adagideli, S. Berber, D. Tomanek, and K. Richter, Phys. Rev. Lett. **100**, 177207 (2008).
[27] Y. Hancock, K. Saloriutta, A. Uppstu, A. Harju, and M. J. Puska, J. Low Temp. Phys. **153**, 393 (2008).
[28] T. Wassmann, A. P. Seitsonen, A. M. Saitta, M. Lazzeri, and F. Mauri, Phys. Rev. Lett. **101**, 096402 (2008).
[29] C. A. Stafford and S. Das Sarma, Phys. Rev. Lett. **72**, 3590 (1994).
[30] C. Stampfer, J. Güttinger, S. Hellmüller, F. Molitor, K. Ensslin, and T. Ihn, Phys. Rev. Lett. **102**, 056403 (2009).